A

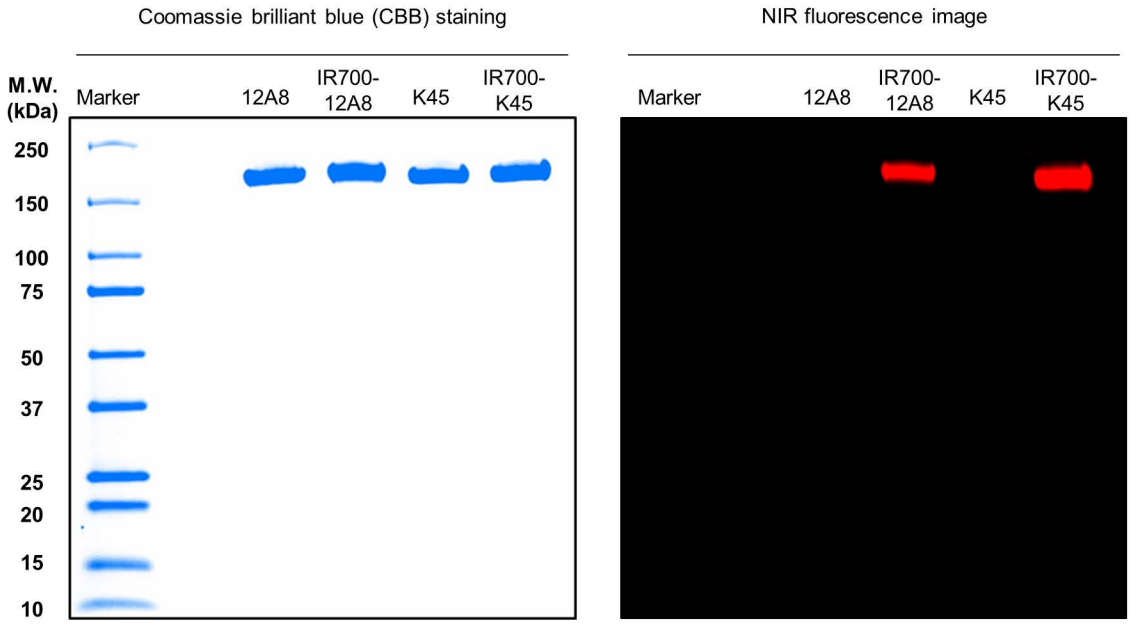
Coomassie brilliant blue (CBB) staining
NIR fluorescence image
M.W. (kDa)
Marker
12A8
IR700-12A8
K45
IR700-K45
250
150
100
75
50
37
25
20
15
10

B

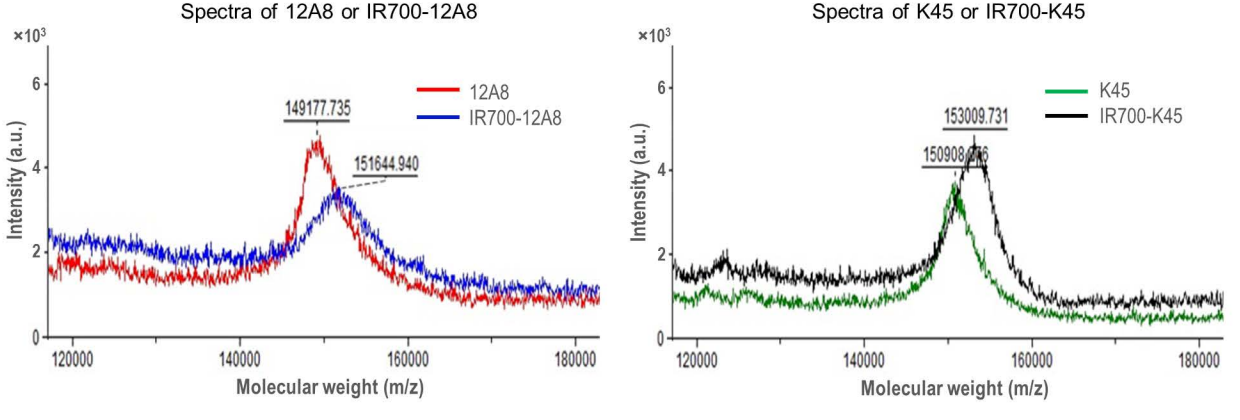
Spectra of 12A8 or IR700-12A8
×10³
Intensity (a.u.)
12A8
IR700-12A8
149177.735
151644.940
Molecular weight (m/z)
Spectra of K45 or IR700-K45
K45
IR700-K45
153009.731
120000
140000
160000
180000

Figure S2

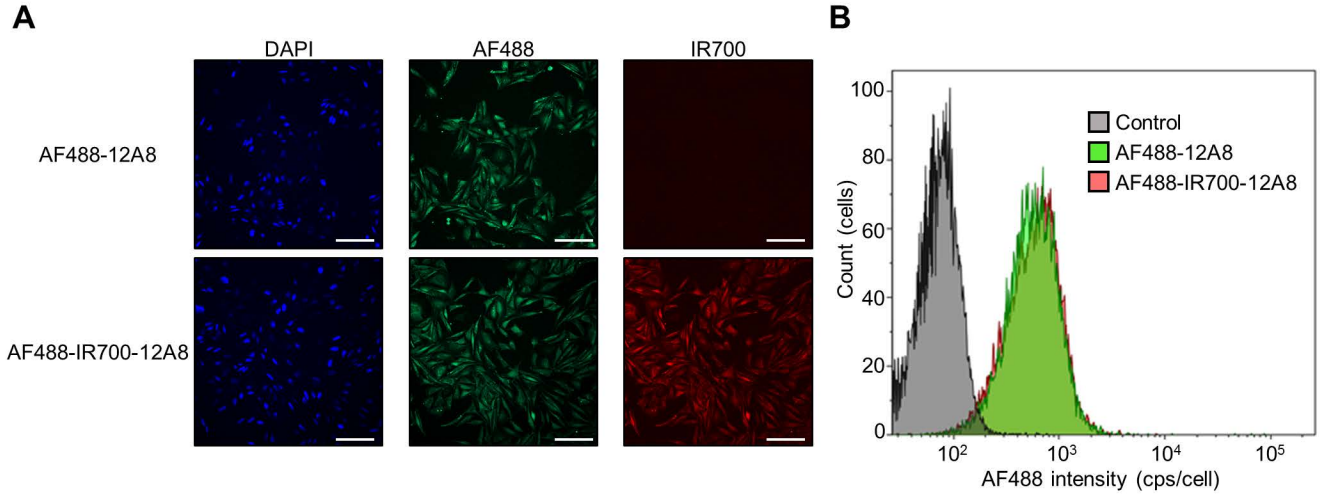
A
DAPI
AF488
IR700
AF488-12A8
AF488-IR700-12A8
B
Control
AF488-12A8
AF488-IR700-12A8
Count (cells)
AF488 intensity (cps/cell)

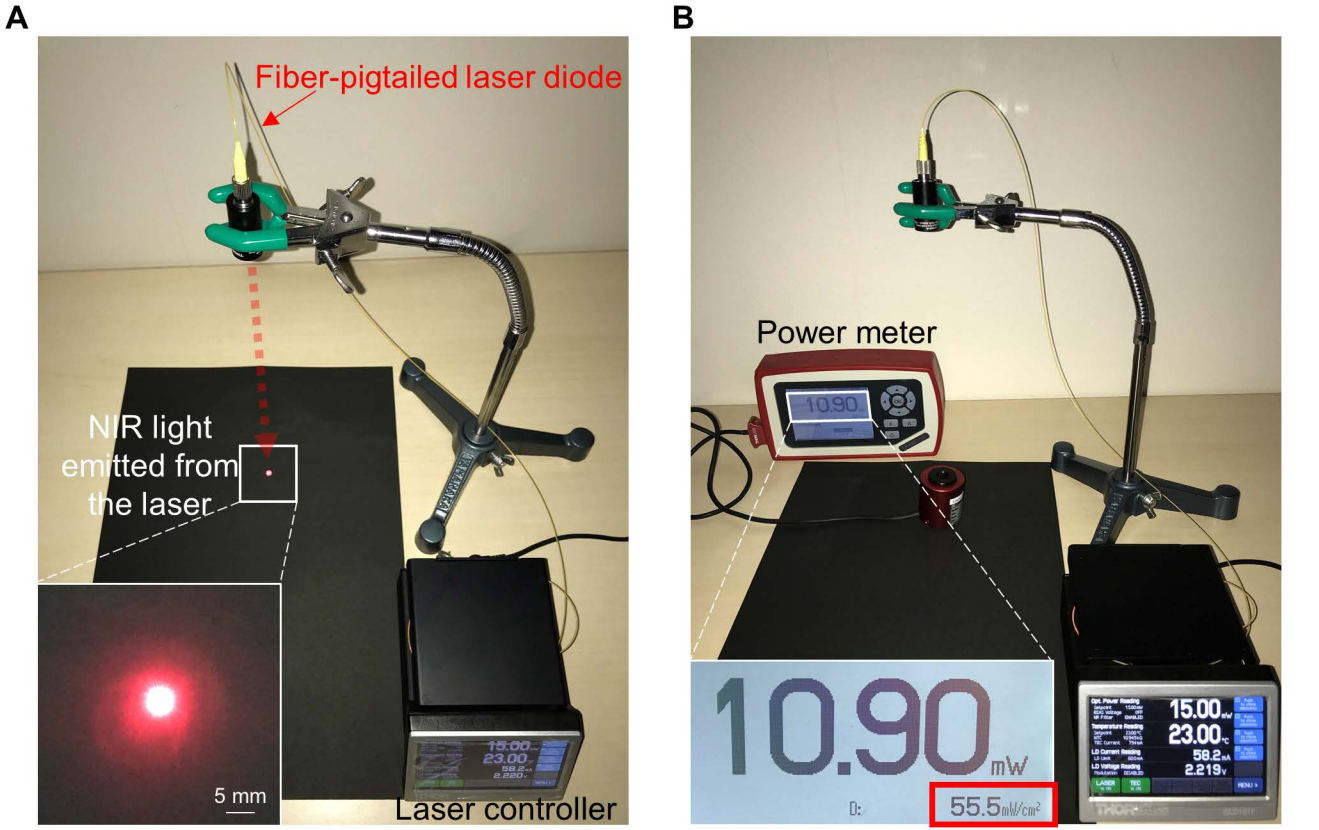
A
Fiber-pigtailed laser diode
NIR light
emitted from
the laser
5 mm
Laser controller
B
Power meter
10.90
mW
55.5mW/cm²
15.00mW
23.00°C
58.2nA
2.219V

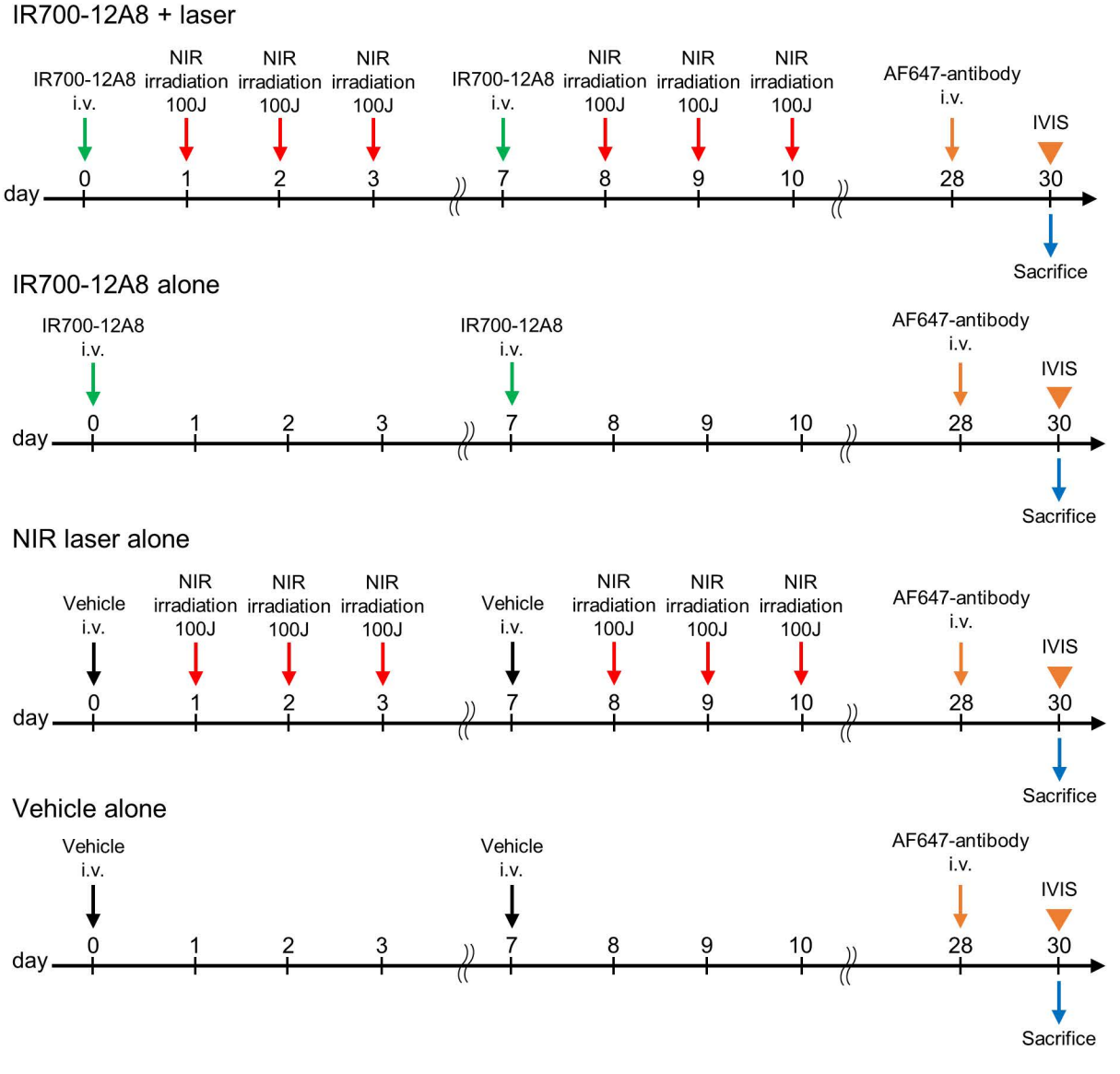
IR700-12A8 + laser
IR700-12A8 i.v.
NIR irradiation 100J
NIR irradiation 100J
NIR irradiation 100J
IR700-12A8 i.v.
NIR irradiation 100J
NIR irradiation 100J
NIR irradiation 100J
AF647-antibody i.v.
IVIS
day
0 1 2 3 7 8 9 10 28 30
Sacrifice
IR700-12A8 alone
IR700-12A8 i.v.
IR700-12A8 i.v.
AF647-antibody i.v.
IVIS
day
0 1 2 3 7 8 9 10 28 30
Sacrifice
NIR laser alone
Vehicle i.v.
NIR irradiation 100J
NIR irradiation 100J
NIR irradiation 100J
Vehicle i.v.
NIR irradiation 100J
NIR irradiation 100J
NIR irradiation 100J
AF647-antibody i.v.
IVIS
day
0 1 2 3 7 8 9 10 28 30
Sacrifice
Vehicle alone
Vehicle i.v.
Vehicle i.v.
AF647-antibody i.v.
IVIS
day
0 1 2 3 7 8 9 10 28 30
Sacrifice

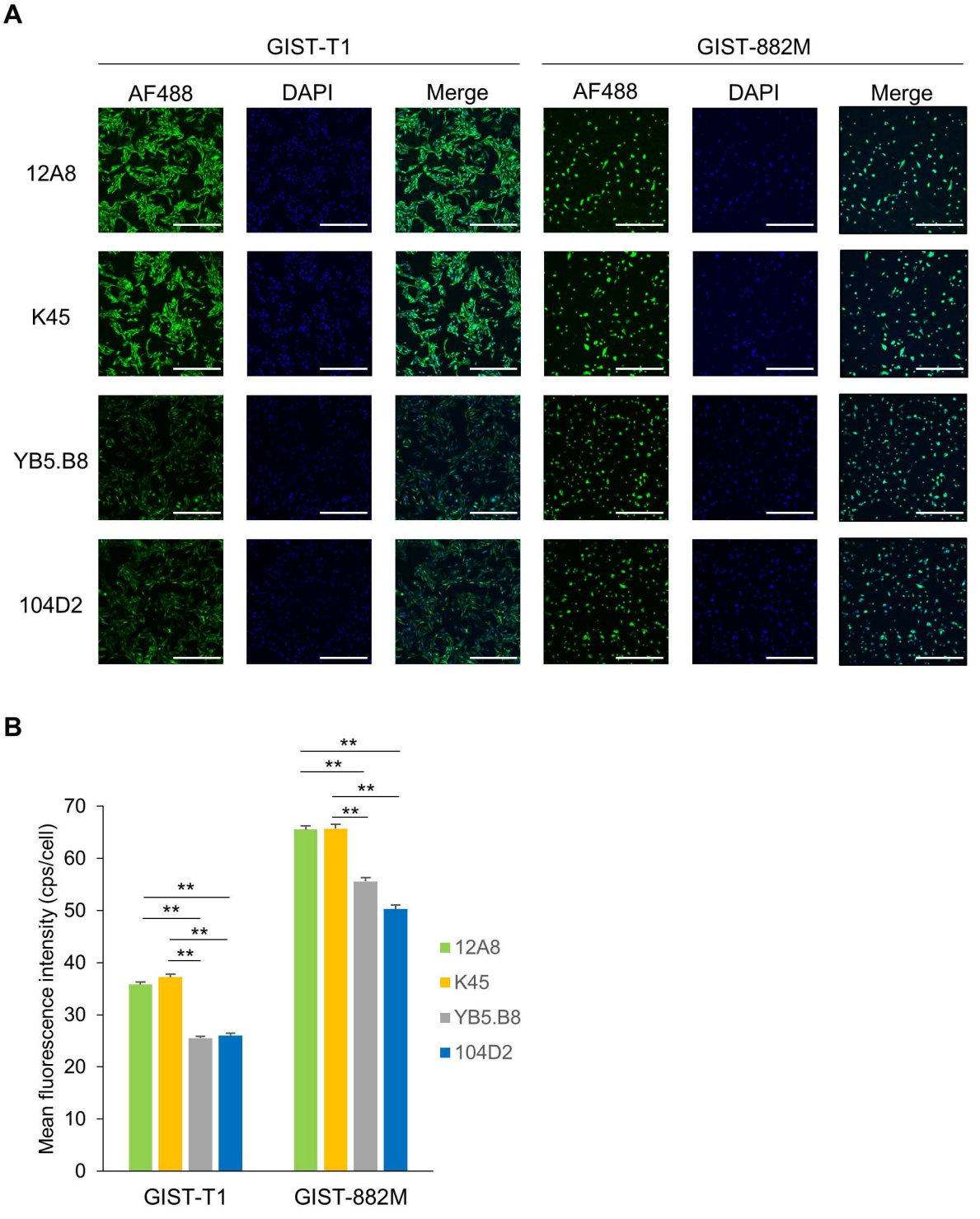
A
GIST-T1
GIST-882M
AF488
DAPI
Merge
AF488
DAPI
Merge
12A8
K45
YB5.B8
104D2
B
Mean fluorescence intensity (cps/cell)
70
60
50
40
30
20
10
0
**
**
**
**
**
**
**
**
12A8
K45
YB5.B8
104D2
GIST-T1
GIST-882M

Figure S6

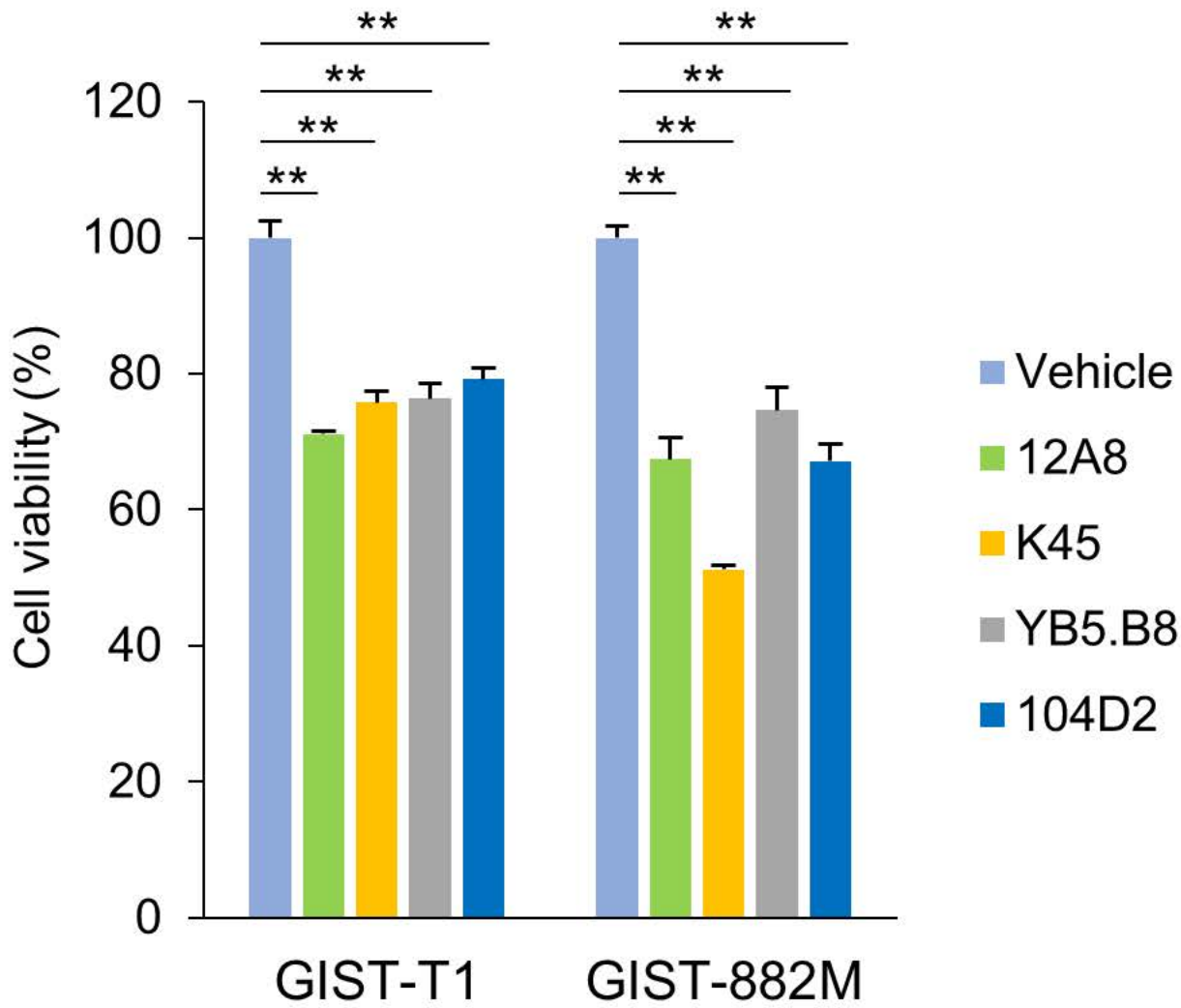
**
**
**
**
**
**
**
**
120
100
80
60
40
20
0
Cell viability (%)
GIST-T1
GIST-882M
Vehicle
12A8
K45
YB5.B8
104D2

Figure S7

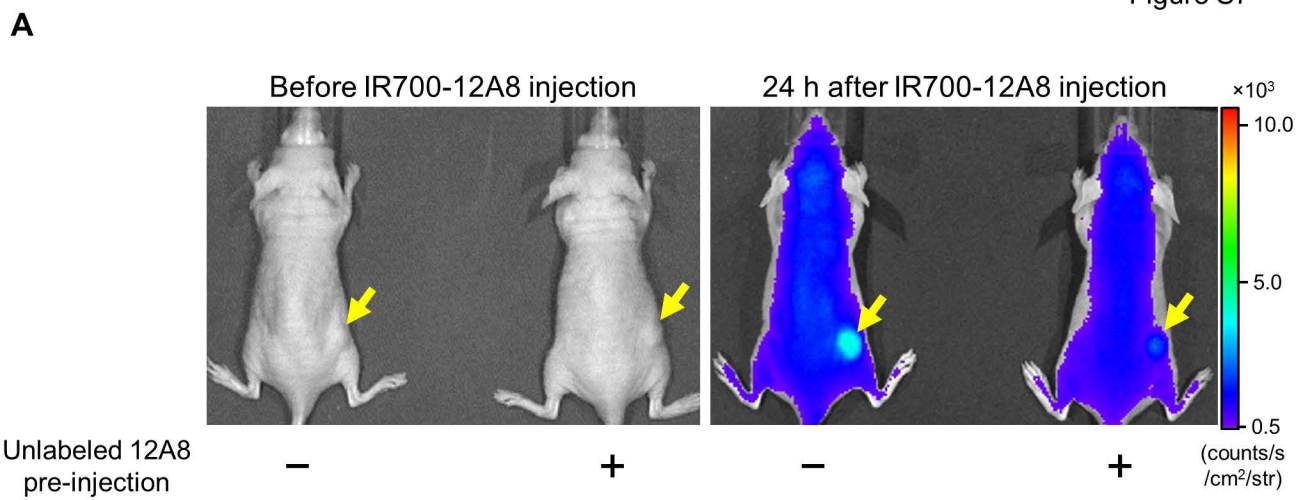
A
Before IR700-12A8 injection
24 h after IR700-12A8 injection
×10³
10.0
5.0
0.5
(counts/s /cm²/str)
Unlabeled 12A8 pre-injection
–
+
–
+

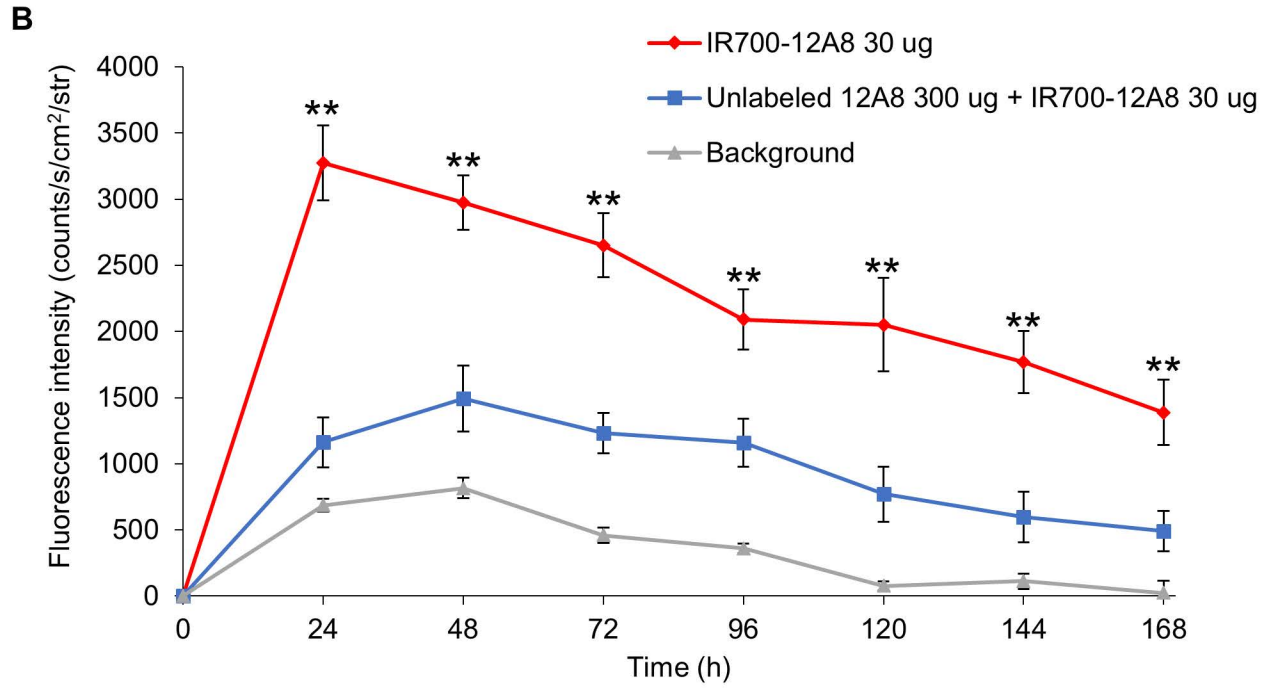
B
IR700-12A8 30 ug
Unlabeled 12A8 300 ug + IR700-12A8 30 ug
Background
Fluorescence intensity (counts/s/cm²/str)
4000
3500
3000
2500
2000
1500
1000
500
0
**
0
24
48
72
96
120
144
168
Time (h)

Figure S8

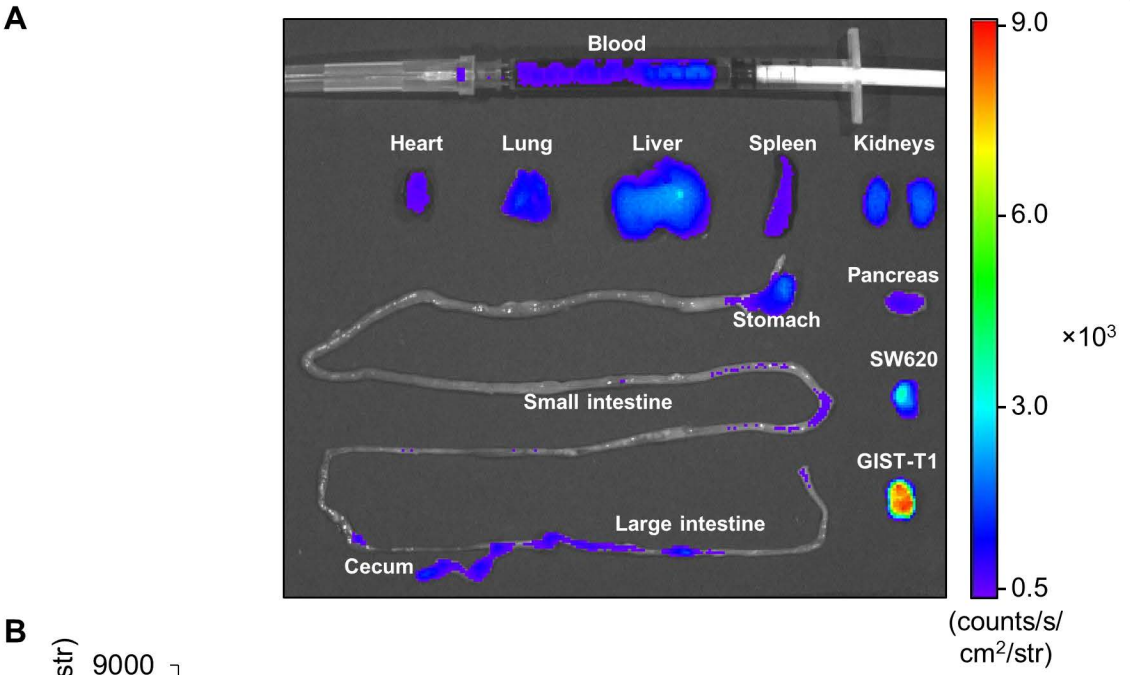
A
Blood
Heart
Lung
Liver
Spleen
Kidneys
Pancreas
Stomach
SW620
Small intestine
GIST-T1
Large intestine
Cecum
9.0
6.0
3.0
0.5
×10³
(counts/s/cm²/str)

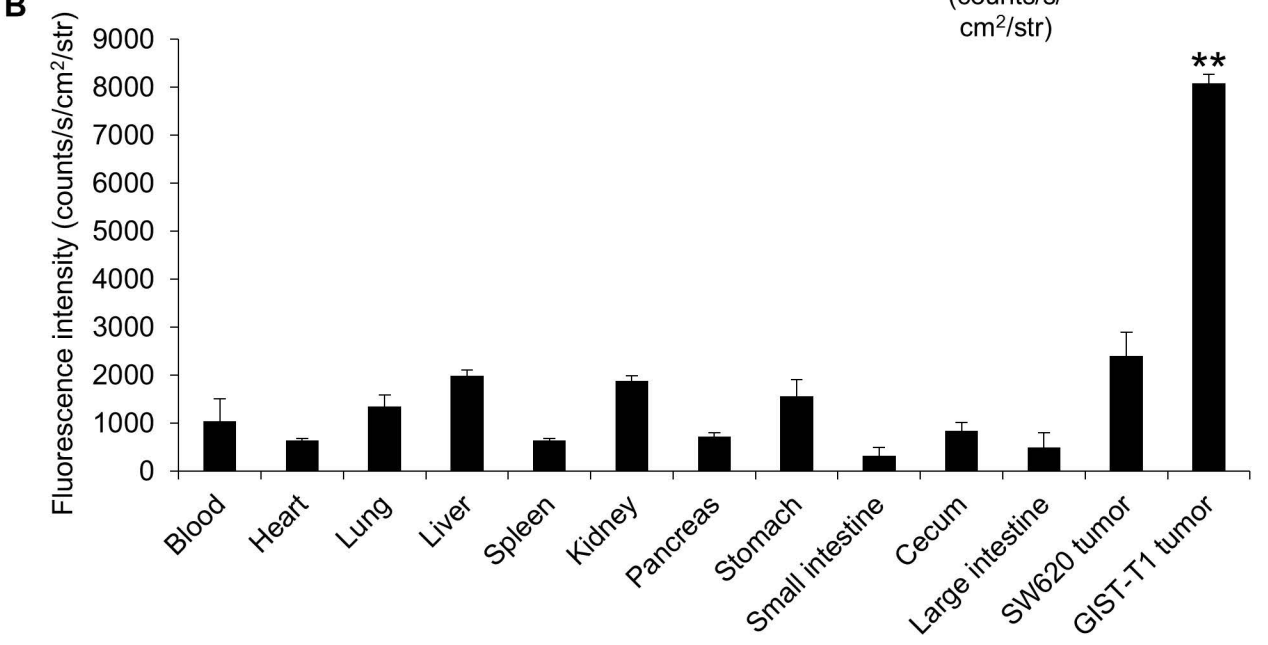
B
Fluorescence intensity (counts/s/cm²/str)
9000
8000
7000
6000
5000
4000
3000
2000
1000
0
**
Blood
Heart
Lung
Liver
Spleen
Kidney
Pancreas
Stomach
Small intestine
Cecum
Large intestine
SW620 tumor
GIST-T1 tumor

Figure S9

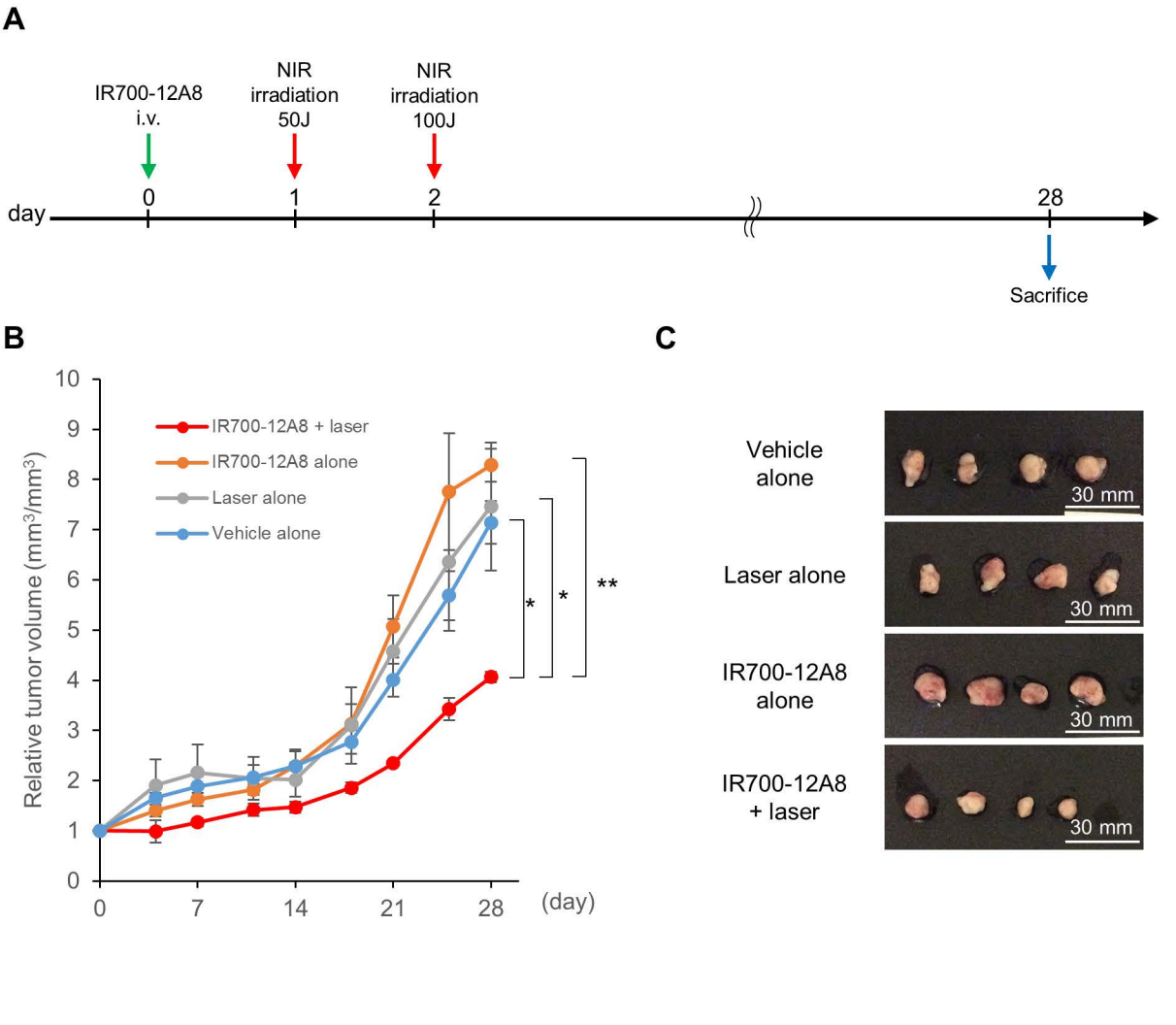
A
IR700-12A8
i.v.
NIR
irradiation
50J
NIR
irradiation
100J
day
0
1
2
28
Sacrifice
B
Relative tumor volume (mm3/mm3)
IR700-12A8 + laser
IR700-12A8 alone
Laser alone
Vehicle alone
*
*
**
(day)
C
Vehicle
alone
Laser alone
IR700-12A8
alone
IR700-12A8
+ laser
30 mm

Figure S10

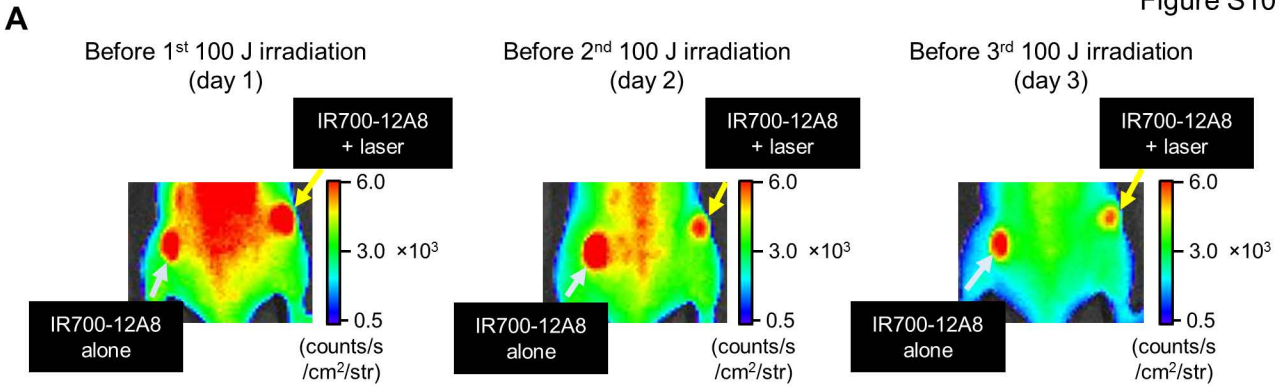
A
Before 1st 100 J irradiation
(day 1)
Before 2nd 100 J irradiation
(day 2)
Before 3rd 100 J irradiation
(day 3)
IR700-12A8
+ laser
IR700-12A8
alone
6.0
3.0 ×10³
0.5
(counts/s
/cm²/str)

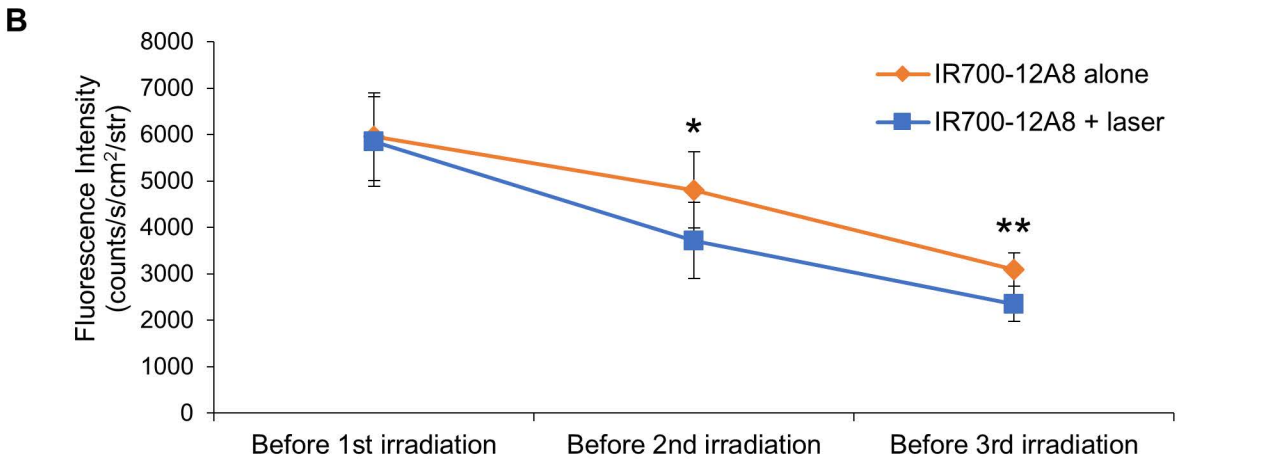
B
Fluorescence Intensity
(counts/s/cm²/str)
8000
7000
6000
5000
4000
3000
2000
1000
0
IR700-12A8 alone
IR700-12A8 + laser
*
**
Before 1st irradiation
Before 2nd irradiation
Before 3rd irradiation

Figure S11

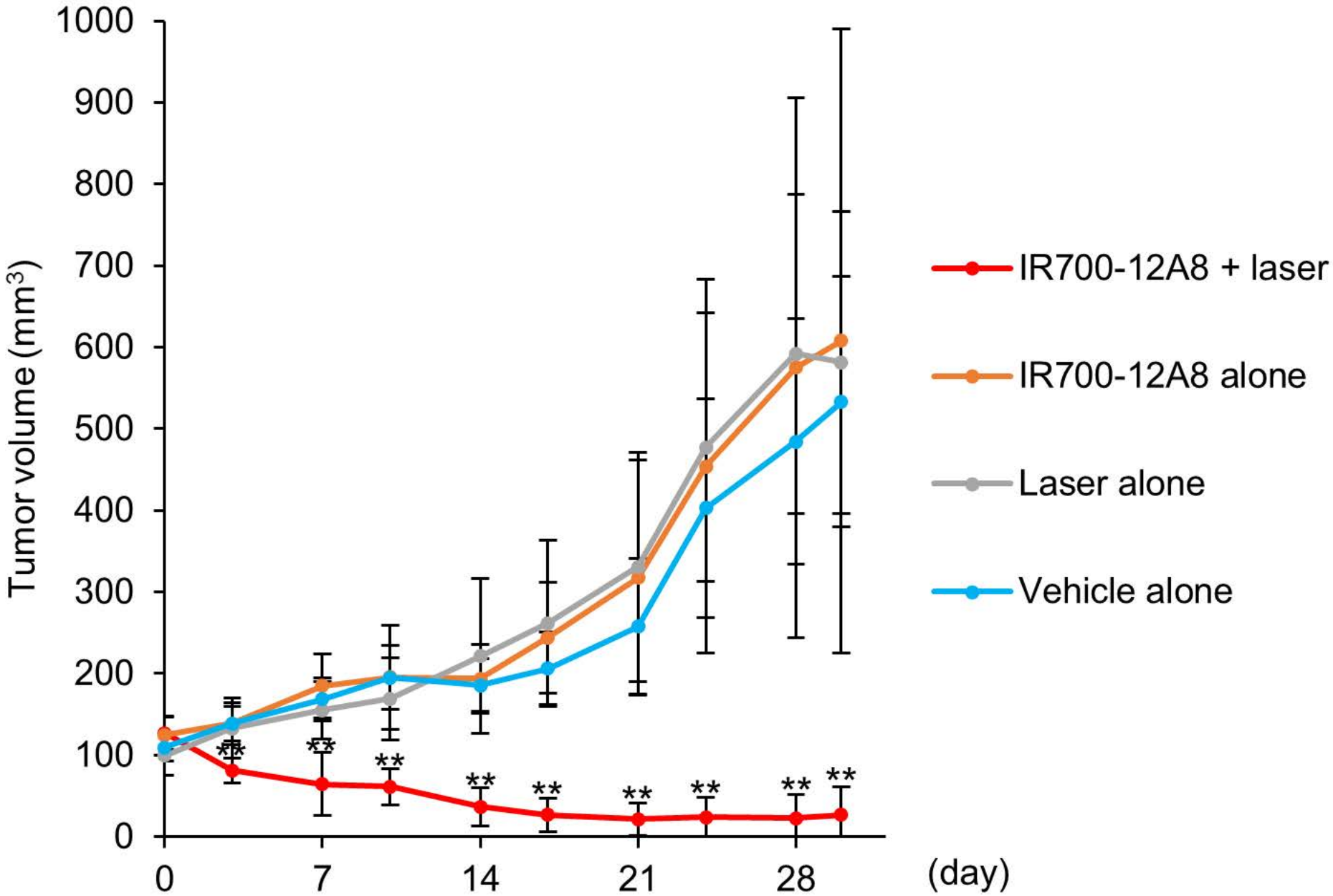
Tumor volume (mm3)
1000
900
800
700
600
500
400
300
200
100
0
0
7
14
21
28
(day)
**
IR700-12A8 + laser
IR700-12A8 alone
Laser alone
Vehicle alone

Figure S12

A Temperature change in vitro (cells)

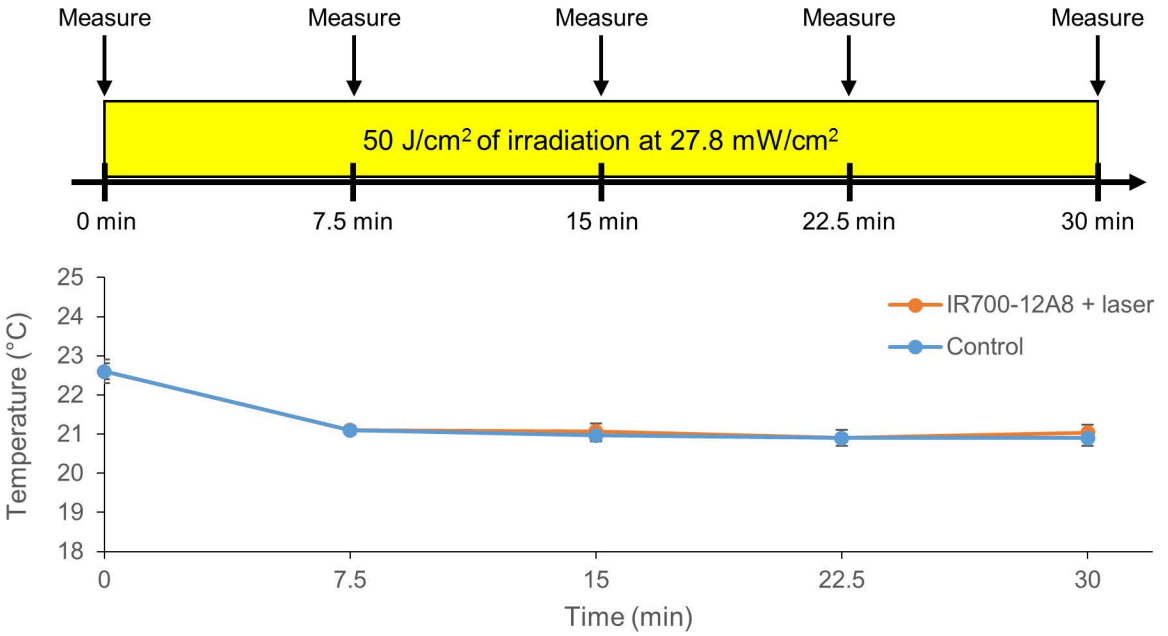

B Temperature change in vivo (mice)

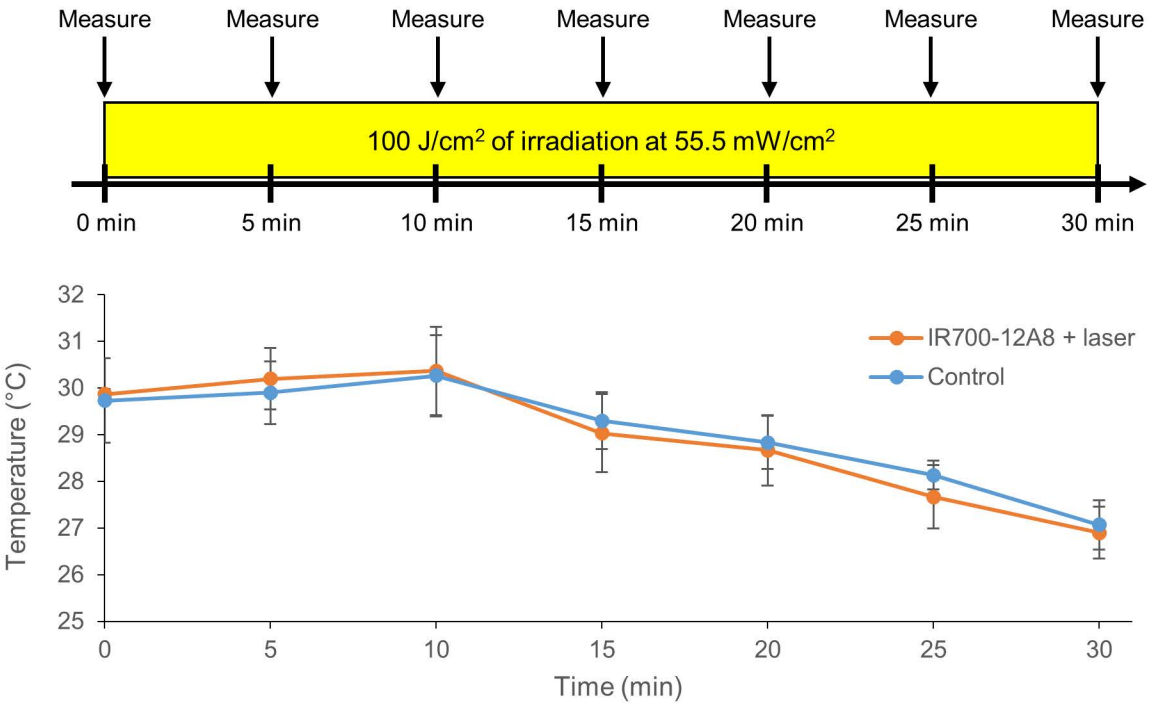

Figure S13

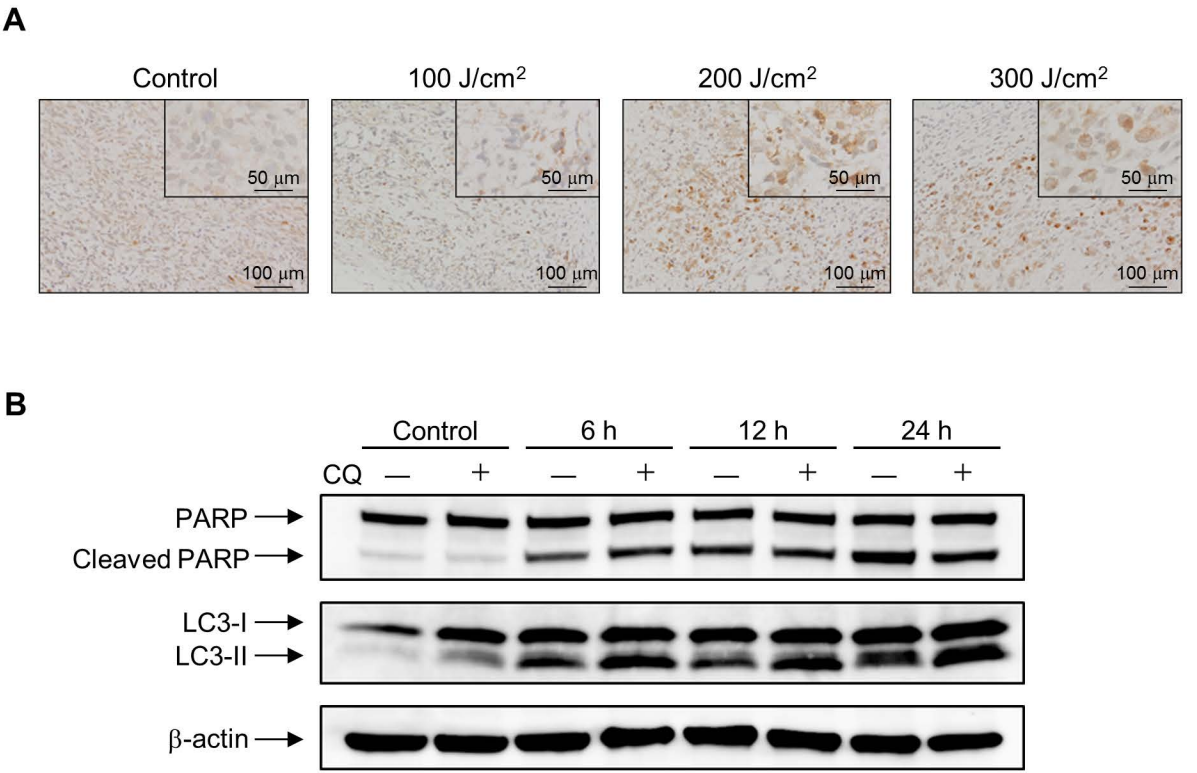
A
Control
100 J/cm2
200 J/cm2
300 J/cm2
50 μm
100 μm
B
Control
6 h
12 h
24 h
CQ — + — + — + — +
PARP
Cleaved PARP
LC3-I
LC3-II
β-actin

Supplementary Figure Legends

Figure S1. Characterization of IR700-labeled 12A8 or K45 antibody by sodium dodecyl sulfate-polyacrylamide gel electrophoresis (SDS-PAGE) and matrix-assisted laser desorption/ionization time-of-flight mass spectrometry (MALDI-TOF MS) analysis. (A) Non-reducing SDS-PAGE analysis of IR700-labedled 12A8 or K45 antibody. Coomassie brilliant blue (CBB) staining revealed a clear single band of unlabeled or labeled 12A8 and K45 antibodies at approximately 150 kDa. Moreover, NIR fluorescence imaging of this gel exhibited a clear single band of IR700-labeled 12A8 or IR700-labeled K45 at the corresponding location (approximately 150 kDa). (B) MALDI-TOF spectra of unlabeled 12A8, IR700-12A8, unlabeled K45, and IR700-K45. The unlabeled 12A8 showed a peak at approximately 150,000 (m/z), and the IR700-labeled 12A8 showed a peak at a slightly higher molecular weight compared with unlabeled 12A8 antibody. Likewise, the IR700-labeled K45 showed a peak at a slightly higher molecular weight compared with unlabeled K45 antibody. The results strongly suggest that the antibodies had been properly labeled and prepared.

Figure S2. Affinity of AF488-conjugated 12A8 (AF488-12A8) and IR700-conjugated AF488-12A8 (IR700-AF488-12A8) for c-KIT on GIST cells. (A) Immunofluorescence staining of GIST-T1 cells with AF488-conjugated 12A8 (AF488-12A8) or IR700-conjugated AF488-12A8 (IR700-AF488-12A8). Nuclei were stained with DAPI (scale bar, 100 μm). (B) Flow cytometric analysis for evaluating the fluorescence intensity of AF488 in GIST-T1 cells stained with

AF488-12A8 (green), AF488-IR700-12A8 (red), and non-staining control (gray). Mean fluorescence intensities in the cells with AF488-12A8 and IR700-AF488-12A8 were 659.0 ± 9.3 a.u. and 649.6 ± 1.9 a.u., respectively, indicating that IR700 conjugation did not essentially change affinity for c-KIT.

Figure S3. Laser devices used in this study. (A) NIR light with a diameter of 5 mm was emitted from a fiber-pigtailed laser diode (LP685-SF15, Thorlabs Inc., Newton, NJ). The red dashed arrow indicates NIR light emission from the laser diode to the irradiated object. (B) Power density was measured with an optical power meter (PM 100, Thorlabs). When we irradiated GIST tumors with NIR light, the power meter showed a power density of 55.5 mW/cm^2.

Figure S4. Treatment protocol for in vivo IR700-conjugated anti-c-KIT antibody (IR700-12A8) combined with NIR laser irradiation therapy for groups of mice receiving IR700-12A8 + laser, IR700-12A8 alone, NIR laser alone, and vehicle alone. Mice were injected with IR700-12A8 or vehicle on day 0 and day 7, and NIR laser irradiation was performed on days 1, 2, 3, 8, 9, and 10. Mice were injected with Alexa Fluor 647-conjugated anti-c-KIT antibody (AF647-antibody) at day 28 for observation of the tumor using the IVIS Spectrum at day 30. The mice were then sacrificed for histological analysis.

Figure S5. Immunofluorescence staining of GIST cells using 4 types of anti-c-KIT monoclonal antibodies. (A) Representative staining patterns of GIST-T1 and GIST-882M cells for c-KIT. The cells were incubated with each

anti-c-KIT antibody (12A8, K45, YB5.B8, or 104D2; 4 μg/mL) as the primary antibody, and then incubated with AF488-conjugated antibody (green) as the secondary antibody. Nuclei were stained with DAPI (blue) and the cells were observed under confocal laser microscopy (original magnification, ×100) (scale bar, 500 μm). (B) Mean fluorescence intensity of AF488 in individual cells incubated with each anti-c-KIT antibody. The mean fluorescence intensity of AF488 was quantified using Image J software. At least 100 cells were quantified for each cell line and each experiment was repeated 3 times. Data represent mean ± standard deviation (SD) (**p<0.01).

Figure S6. Growth inhibitory effect of anti-c-KIT antibodies on GIST cells. The cells were incubated with each anti-c-KIT antibody (12A8, K45, YB5.B8, or 104D2; 20 μg/mL) at 37°C for 6 days, and cell viability was assessed by WST-8 assay. Data represent mean ± SD (n=3, **p<0.01).

Figure S7. Competition assay of IR700-12A8 fluorescence imaging with unlabeled 12A8 in GIST-T1-xenografted mice. (A) Representative fluorescence images of mice injected with IR700-12A8 (30 μg) alone (left), or pre-injected with unlabeled 12A8 (300 μg) and injected with IR700-12A8 (30 μg) (right). The yellow arrows indicate GIST-T1 tumors. The tumor from a mouse pre-injected with unlabeled 12A8 showed a faint fluorescent signal, whereas the tumor from a mouse treated with vehicle alone showed a clear fluorescent signal 24 h after IR700-12A8 injection. (B) Chronological changes in the mean fluorescence intensity in GIST-T1 tumors. The mean fluorescence intensity of the tumor in the

pre-injected mouse was significantly lower than that in mice treated with vehicle alone at all timepoints. Data represent mean ± SD (n=3, **p<0.01).

Figure S8. Ex vivo fluorescent imaging of xenografted GIST-T1 and SW620 tumors and of various organs from a mouse injected with IR700-12A8. (A) Representative ex vivo images of tumors and organs resected at 120 h after injection. The GIST-T1 tumor showed a strong fluorescent signal, whereas the SW620 tumor, liver, and kidney showed weak fluorescent signals. (B) The mean fluorescence intensities of the tumors and organs. The respective fluorescence intensities in GIST-T1 tumors, SW620 tumors, liver, and kidney were 8083 ± 190, 2405 ± 484, 1985 ± 119 and 1885 ± 98 a.u.. Data represent mean ± SD (n=3, **p<0.01).

Figure S9. Preliminary study of in vivo IR700-12A8-mediated PIT for GIST-xenografted mice. (A) Treatment regimen for IR700-12A8 injection and NIR light irradiation. Mice were injected with IR700-12A8 (100 μg) at day 0 and the tumors were irradiated with 50 J/cm^2 of NIR light at day 1 and 100 J/cm^2 at day 2. The mice were finally sacrificed at day 28. (B) Chronological changes in relative tumor volume in the IR700-12A8 + laser group, IR700-12A8 alone group, laser alone group, and vehicle alone group (n=4 per group). Although the tumors did not regress, tumor growth was significantly suppressed in the IR700-12A8 + laser group as compared with the other groups. Data represent mean ± SD (*p<0.05, **p<0.01). (C) Tumors resected from each group of mice at day 28.

Figure S10. IR700 fluorescent signal in tumors before each NIR light irradiation at day 1, 2, and 3. (A) Representative fluorescence images of the tumors before the first (day 1), second (day 2), and third irradiation (day 3). The left tumor was treated with IR700-12A8 alone and the right tumor was treated with IR700-12A8-mediated NIR irradiation (IR700-12A8 + laser). (B) The mean fluorescence intensity in the tumors before each NIR light irradiation at day 1, 2, and 3. The intensity in the right tumors (IR700-12A8 + laser) was effectively decreased by PIT, whereas that in the left tumors (IR700-12A8 alone) was gradually decreased with fading of fluorescence. The intact fluorescence of IR700 photosensitizer was still present before the second and even the third irradiation. Data represent mean ± SD (n=7, *$p<0.05$, **$p<0.01$).

Figure S11. Chronological changes in absolute tumor volumes in the 4 groups of mice treated with IR700-12A8 + laser, IR700-12A8 alone, laser alone, or vehicle alone.

Figure S12. Temperature changes during irradiation with NIR light in vitro (A) and in vivo (B). (A) GIST-T1 cells in 96-well plates were treated with IR700-12A8 for 6 h and then irradiated with NIR light at 50 J/cm^2 (27.8 mW/cm^2) for 30 min. The temperature of the medium for GIST-T1 cells was measured every 7.5 min during irradiation using a contactless thermometer (MT-7, AS ONE, Osaka, Japan). (B) Mice with GIST-T1 xenograft tumors were injected with IR700-12A8 and the tumors were then irradiated with NIR light at 100 J/cm^2 (55.5 mW/cm^2) for 30 min. The temperature of the tumor was measured every 5 min during

irradiation. Data represent mean ± SD (n=3).

Figure S13. Apoptosis and autophagic activity in GIST-T1 cells after treatment with IR700-12A8 and NIR laser irradiation. (A) Immunohistochemistry for LC3 in sections of tumor treated with 100, 200, and 300 J/cm^2 of IR700-12A8-mediated NIR irradiation in vivo. A rabbit anti-human LC3B monoclonal antibody (D11, Cell Signaling Technology) was used as a primary antibody. Original magnification, × 200. High-magnification images are shown in the inset at the upper right (× 400). (B) Chronological changes in PARP and LC3 expression in GIST-T1 cells after treatment with IR700-12A8-mediated NIR laser irradiation in vitro. The cells were incubated with IR700-12A8 in the presence or absence of 25 μM of chloroquine (CQ) and irradiated by 20 J/cm^2 of NIR light. The expression of PARP and LC3 was evaluated by Western blotting using anti-human PARP polyclonal antibody (Cell Signaling Technology) and D11, respectively, at 6, 12, and 24 h after irradiation. β-actin was used as a loading control.